ARMY RESEARCH LABORATORY

Analytical Prediction of Lower Leg Injury in a Vehicular Mine Blast Event

by Justine Li

ARL-TR-5053 **January 2010**

NOTICES

Disclaimers

The findings in this report are not to be construed as an official Department of the Army position unless so designated by other authorized documents.

Citation of manufacturer's or trade names does not constitute an official endorsement or approval of the use thereof.

Destroy this report when it is no longer needed. Do not return it to the originator.

Army Research Laboratory
Aberdeen Proving Ground, MD 21005-5056

ARL-TR-5053 **January 2010**

Analytical Prediction of Lower Leg Injury in a Vehicular Mine Blast Event

Justine Li
Senior, Department of Aeronautics and Astronautics, MIT

REPORT DOCUMENTATION PAGE	Form Approved OMB No. 0704-0188

1. REPORT DATE *(DD-MM-YYYY)*	2. REPORT TYPE	3. DATES COVERED (From - To)
Janaury 2010	Summary	

4. TITLE AND SUBTITLE	5a. CONTRACT NUMBER
Analytical Prediction of Lower Leg Injury in a Vehicular Mine Blast Event	5b. GRANT NUMBER
	5c. PROGRAM ELEMENT NUMBER
6. AUTHOR(S)	5d. PROJECT NUMBER
Justine Li	5e. TASK NUMBER
	5f. WORK UNIT NUMBER
7. PERFORMING ORGANIZATION NAME(S) AND ADDRESS(ES)	8. PERFORMING ORGANIZATION REPORT NUMBER
U.S. Army Research Laboratory Attn: RDRL-WMT-B Aberdeen Proving Ground MD 21005	ARL-TR-5053
9. SPONSORING/MONITORING AGENCY NAME(S) AND ADDRESS(ES)	10. SPONSOR/MONITOR'S ACRONYM(S)
	11. SPONSOR/MONITOR'S REPORT NUMBER(S)

12. DISTRIBUTION/AVAILABILITY STATEMENT

Approved for public release; distribution unlimited.

13. SUPPLEMENTARY NOTES

14. ABSTRACT

Modeling the effects of anti-vehicular mines on the lower human body through both experiments and finite element models is expensive. The objective of this project is to produce accurate predictions of axial tibia loads through the development and verification of a one-dimensional (1-D) analytical model. In this effort, a 1-D analytical model of the lower leg created in this project was evaluated for its accuracy in predicting the maximum tibia force given a displacement over a period of time. The calculated forces were compared to the experimental data presented in Bir et al. (2006). The analysis shows that the model, which uses only springs, leads to convergence of the calculated maximum tibia force. The ideal number of springs to use in the analytical model is determined by the numerical integration method. Using a simple spring-mass system of variable number of elements, I found that using the two-step Runge-Kutta numerical integration method with 50 springs and a scaling factor dependent on maximum floor velocity is accurate with the experimental data presented for the Hybrid-III 50% Dummy in Bir et al. (2006). Further verification using more experimental data is necessary to confirm the validity of the model.

15. SUBJECT TERMS

Lower leg injury, analytical prediction of axial tibia load, force-deflection curve, numerical integration

16. SECURITY CLASSIFICATION OF:			17. LIMITATION OF ABSTRACT	18. NUMBER OF PAGES	19a. NAME OF RESPONSIBLE PERSON
a. REPORT	b. ABSTRACT	c. THIS PAGE			Rahul Gupta
Unclassified	Unclassified	Unclassified	UU	28	19b. TELEPHONE NUMBER (*Include area code*) (410) 278-6035

Standard Form 298 (Rev. 8/98)
Prescribed by ANSI Std. Z39.18

Contents

List of Figures

List of Tables

Acknowledgments

I would like to thank Dr. Rahul Gupta and Mr. Rob Bitting for their time, space, and patience this summer.

INTENTIONALLY LEFT BLANK.

1. Introduction and Background

The primary purpose of anti-vehicular landmines is to inflict damage on an Army vehicle and its occupants. Since the blast originates from the ground, the occupants experience the full effects of the blast through their lower legs, the part of the body closest to the mine. By studying the effects of anti-vehicular landmines on the human body, modifications may be made to the vehicles to mitigate bodily harm.

The closest simulation of an anti-vehicular landmine detonation is an experiment that uses explosives and human surrogates. The entire setup, including the dummy, sensors, and test stand, is expensive. The experiment could take weeks to prepare, the sensors could fail to read the data, and the dummy, along with everything else, could be destroyed in a single test without collecting useful data. In this sense, it is logical to create a computer model of the events of a landmine event.

The first step in simulating a landmine event is to use a finite element model to find a solution numerically. In this instance, the solution would be the force experienced by the tibia in the vertical direction. However, since a model of the event would require significant computational power, a finite element model would not be ideal for a quick approximation of the problem.

The ultimate objective is to create a simplified computer model that would be cost efficient in approximating the force experienced in the lower leg, which could then be used to determine the resulting leg damage. This report describes in detail the process in which the simplified computer model was developed and its accuracy in predicting the forces experienced by the lower leg in an anti-vehicular landmine blast was verified.

2. Experiment and Calculations

The goal is to relate the floor displacement to lower leg force and verify the analytical solution using the results from testing the Hybrid-III dummy in the Test Rig for Occupant Safety Systems (TROSS) system presented in Bir et al. (2006). Given a floor displacement over a period of time, an analytical model should be able to accurately predict the maximum force experienced by the tibia of the occupant.

2.1 Model

This analytical model uses a series of springs and masses to model the tibia. Beginning with a one-spring, one-mass system, the model has been expanded to calculate the maximum tibia force for a given number of springs and masses (figure 1).

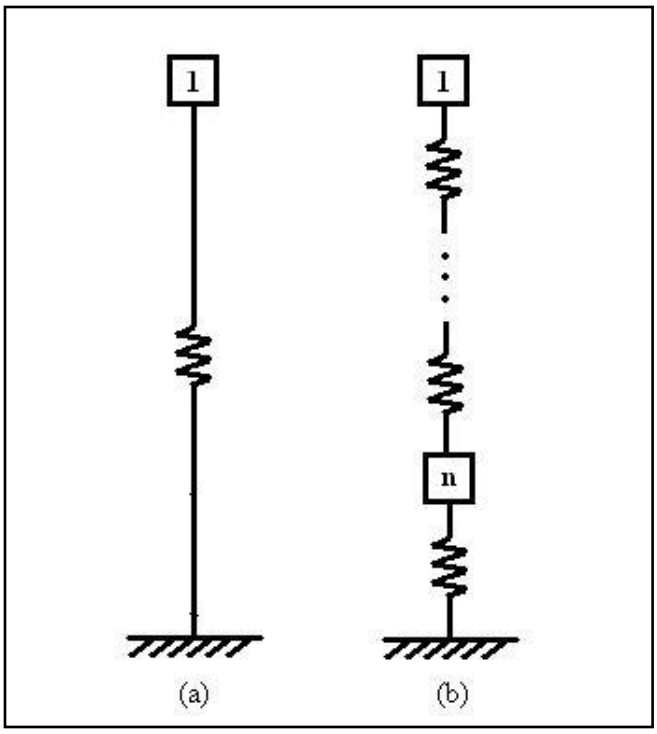

Figure 1. Analytical model, showing a (a) one-mass, one-spring system and (b) an n mass, n spring system.

For the model, the n masses are distributed at constant intervals and labeled from 1 to n starting at the knee and ending at the ankle. The bottom of the boot is rigidly attached to the floor. All n masses have one degree of freedom in the vertical direction. The springs are assumed to be ideal and follow Hooke's Law.

This analytical model uses the SI unit system.

2.2 Calculations

For each mass, the vertical coordinate is calculated using a combination of basic physical concepts and a numerical integration method. The masses are calculated from the geometric parameters provided by the Hybrid-III LS-DYNA model. Since there are a finite number of masses in the model, the tibia mass is discretized into n parts and distributed uniformly.

The initial conditions for the vertical coordinate, vertical velocity, and vertical acceleration are initialized to assumed values. For this model, the vertical coordinates are initially distributed evenly over the length of the tibia given the number of masses desired. Two masses are placed below the tibia, one at the ankle and the other at the heel. Both the vertical velocity and the vertical acceleration are initialized at 0 m/s and 0 m/s^2, respectively. The decision to leave gravity out of the problem is based on the fact that the accelerations the masses experience are an order of magnitude greater than that of gravity.

Using the forward Euler method, the midpoint method, and the two-step Runge-Kutta method for numerical integration, the values for the states for the previous time step were used to extrapolate the value for the states in the current time step. In order to calculate the vertical acceleration for each of the masses, a basic force diagram was used, resulting in the following equations:

Node 1: Knee: $$m_1 y_1'' = k(l_1 - (y_1 - y_2)) \quad (1)$$

Nodes 2 to n-1: Intermediate: $$m_i y_i'' = k(l_i - (y_i - y_{i+1})) - k(l_{i-1} - (y_{i-1} - y_i)) \quad (2)$$

Node n: Ankle: $$m_n y_n'' = k(l_n - (y_n - y_{floor})) - k(l_{n-1} - (y_{n-1} - y_n)) \quad (3)$$

where l_i= original length of spring i, and y_i = vertical coordinate of mass i.

Using Hooke's Law and the deformation of the tibia in the vertical direction, the total force on the tibia for each time step is calculated.

Since the model does not implement dampers, the results from this analysis oscillate. The maximum tibia force value is the first local maximum of the force vs. time graph.

2.3 MATLAB Script

Given a *.dat file for the floor displacement over a certain period of time, MATLAB loads the data into a matrix. From this file, the time and corresponding floor displacement are stored in column arrays. The number of masses is stored in the variable n, and the masses and lengths of the tibia and femur are stored in variables as well.

Using three matrices, the state variables, vertical coordinate, vertical velocity, and vertical acceleration are stored for each mass and each time step. An iterative loop is used to populate the matrices with the appropriate value calculated via the method described in section 2.2.

3. Results and Discussion

In order to verify that the analytical model created in MATLAB, two sets of simulated data were produced from an LS-DYNA simulation of a detonation occurring beneath a plate. The simulated results are compared to the experimental data provided in Bir et al. (2006). Running the script using the original data with two springs led to the results listed in table 1.

Table 1. Values calculated from simulated data using analytical two-spring model.

Data File	Max Displacement (m)	Max Velocity (m/s)	Max Tibia Force (N)
Disp2.dat	0.7910	244.3158	3,081,000
Disp3.dat	0.3555	45.8794	371,100

Since both of the simulated data sets provided maximum floor displacements and maximum velocities that do not lie within the range of the experimental values, the data sets were scaled to provide a maximum floor displacement within the range of the experimental data. The script was run again with two springs and a scaling factor for each of the two data sets (table 2).

Table 2. Values calculated from the scaled simulated data using analytical two-spring model.

Data File	Scale	Max Displacement (m)	Max Velocity (m/s)	Max Tibia Force (N)
Disp2.dat	1/46	0.0172	5.3112	66,970
Disp3.dat	1/21	0.0169	2.1847	17,670

From this analysis using the forward Euler method of numerical integration, it may be noted that the scaled data from DISP3, in terms of maximum displacement and maximum velocity, most accurately matches the experimental data. For the rest of the analysis, only 1/21-scaled DISP3 data were used for the purposes of verification. Despite similar values for displacement and velocity, the maximum tibia force was over two times that of the experimental data.

In the second round of analysis, using only the 1/21-scaled DISP3 data, the tibia force was computed using 2 to 8 springs with distributed masses along the length of the tibia. Figure 2 shows the tibia force versus time for the 9-spring, forward Euler analytical model.

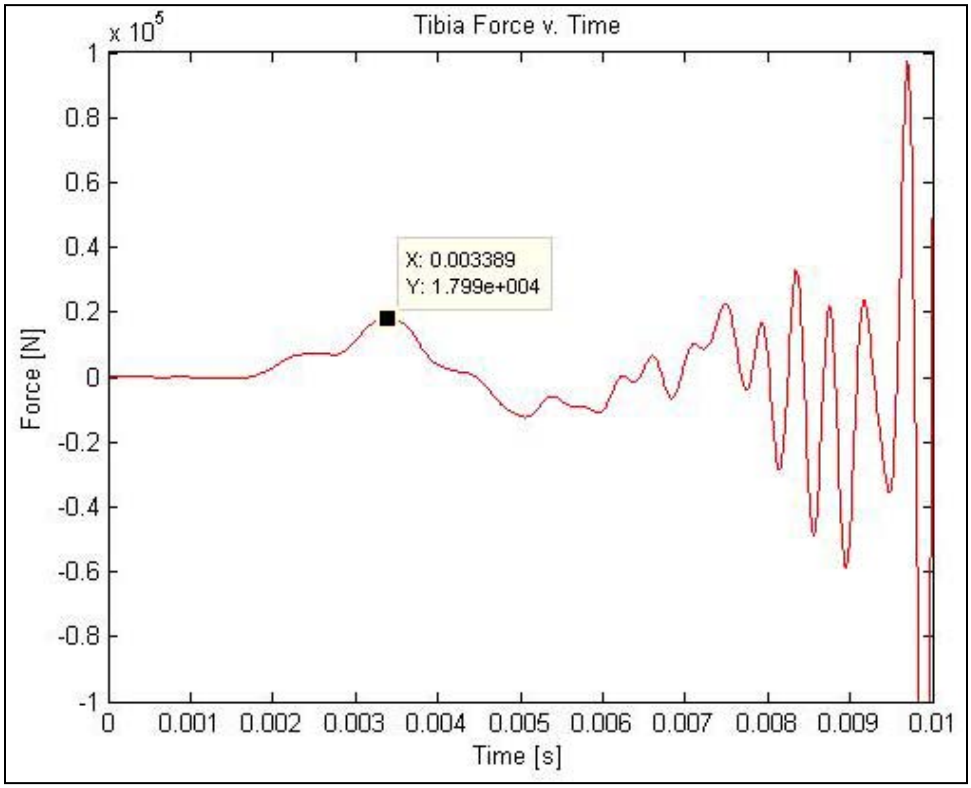

Figure 2. Tibia force versus time for the 9-spring, forward Euler analytical model.

As the tibia is further divided into more springs and masses, the oscillatory behavior masks the first maximum tibia force, so the maximum number of springs and masses that may be used in the analytical model is 8.

The solution to the n-spring model is then calculated using the midpoint method for numerical integration. The oscillatory behavior that appeared in the 9-spring forward Euler model appeared in the 27-spring model using the midpoint method, allowing for the tibia mass to be more distributed throughout the model. It can be noted in figure 3 that using the midpoint method and an increased number of masses leads to a 2.72% decrease in the maximum tibia force as well as a decrease in the amplitude of oscillations.

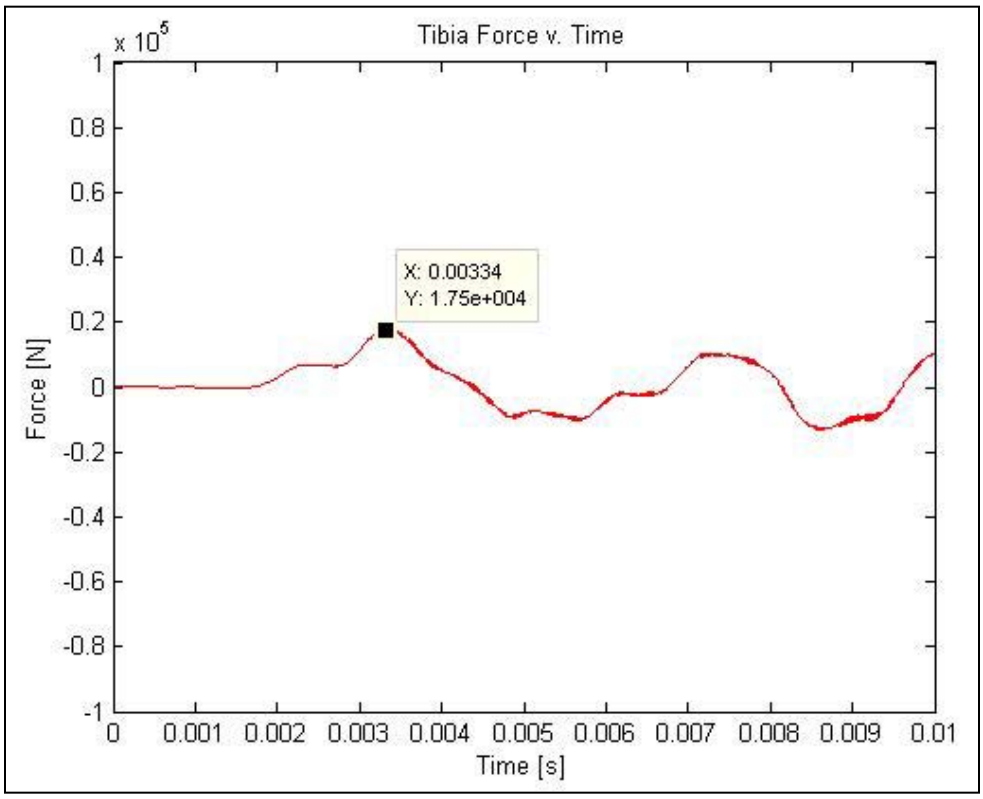

Figure 3. Tibia force versus time for the 27-spring, midpoint method analytical model.

Using an implicit numerical method, the n-spring model allows for an unlimited distribution of masses and number of springs in the model. The use of the two-step Runge-Kutta numerical integration method leads to a further decrease of 0.34% in maximum tibia force and eliminates the residual oscillations seen in both the forward Euler and midpoint method solutions. Increasing the number of nodes beyond 50 (figure 4) proved to be relatively time-expensive and unnecessary since the solution converged with this many nodes.

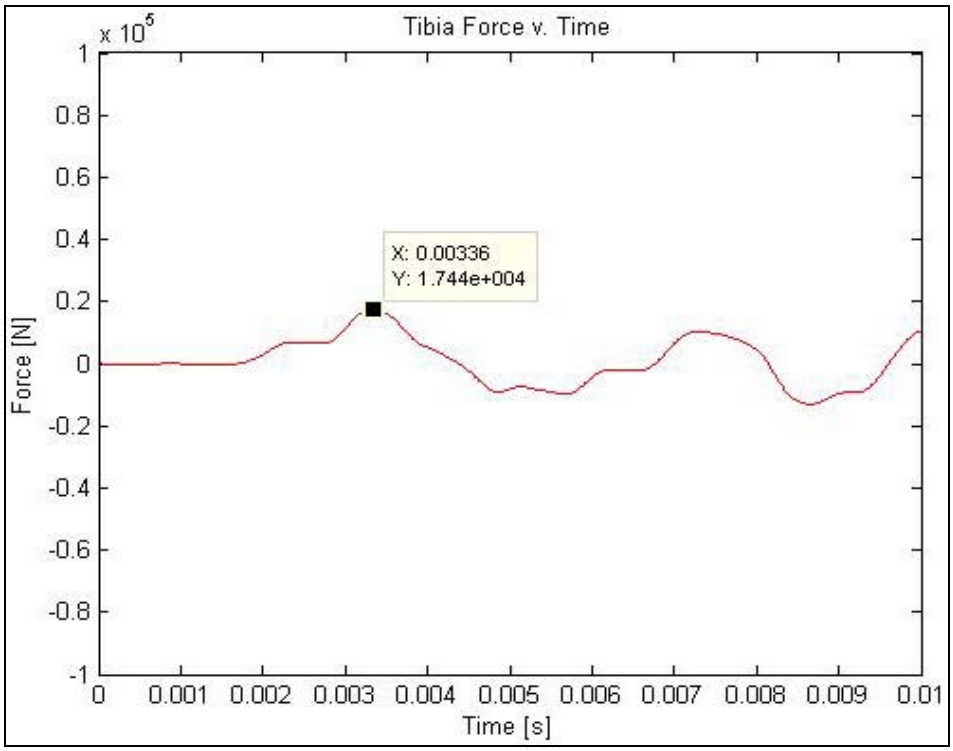

Figure 4. Tibia force versus time for the 50-spring, two-step Runge-Kutta method analytical model.

In figure 5, it can be seen that as the number of springs increases in the midpoint method and the two-step Runge-Kutta models, the calculated maximum tibia force converges. However, the calculated force is approximately twice the experimental maximum tibia force experienced without boots.

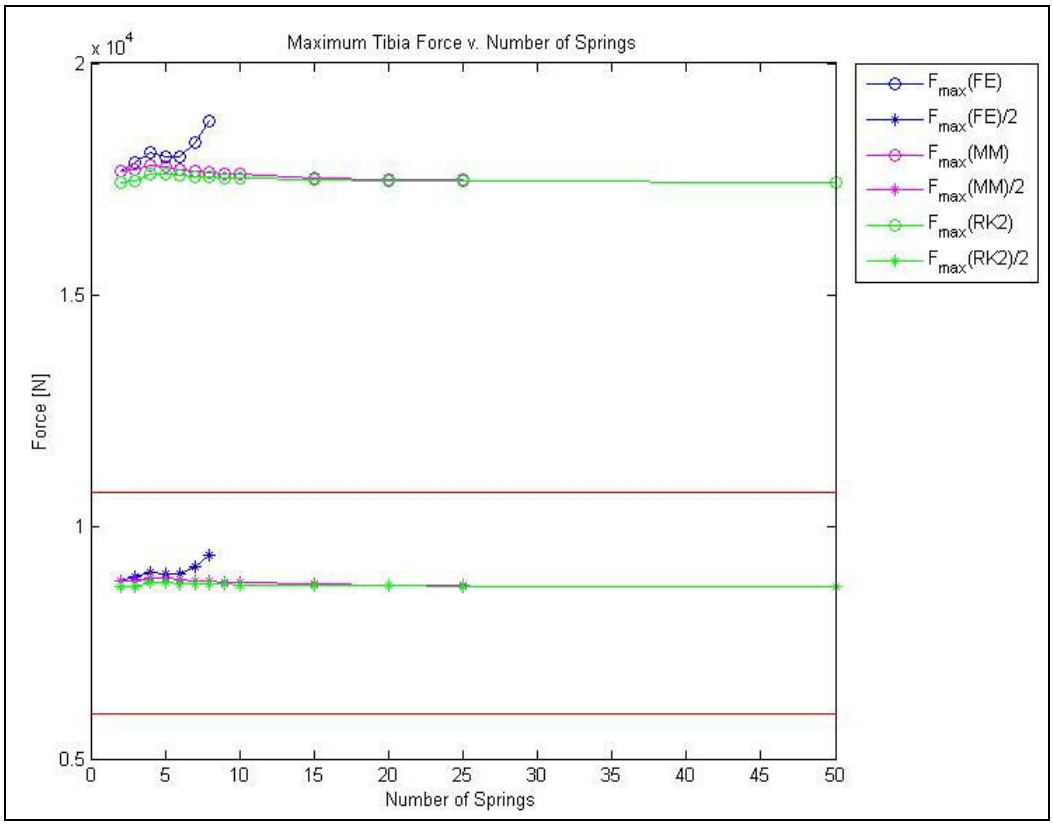

Figure 5. Force versus number of springs for different numerical methods.

Note: The lines show minimum and maximum no boot maximum tibia force from the Bir et al. (2006) measurements.

In figures 6 and 7, the calculated force maximums from DISP3 very nearly match experimental data, while the force maximums calculated from DISP2 demonstrate that the floor displacement data resulted from a much more severe blast than experienced in the TROSS experiment.

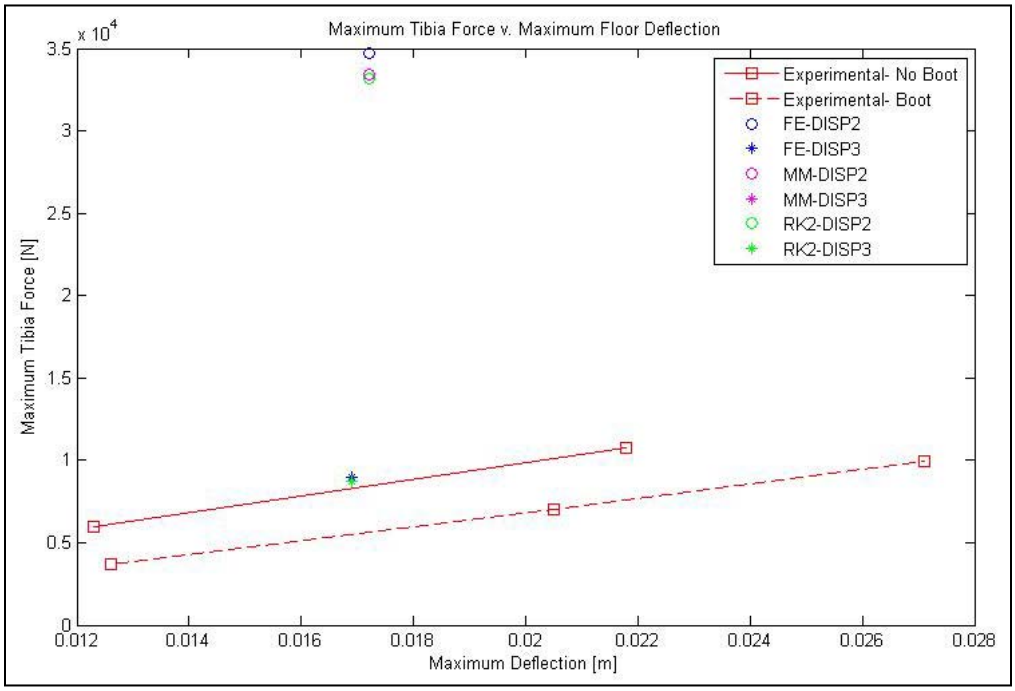

Figure 6. Scaled maximum tibia force versus maximum floor deflection .

Note: For both figures 6 and 7, the data points shown use different numbers of springs in the model; the FE model uses 5 springs, the MM model uses 26 springs, and the RK2 model uses 50 springs.

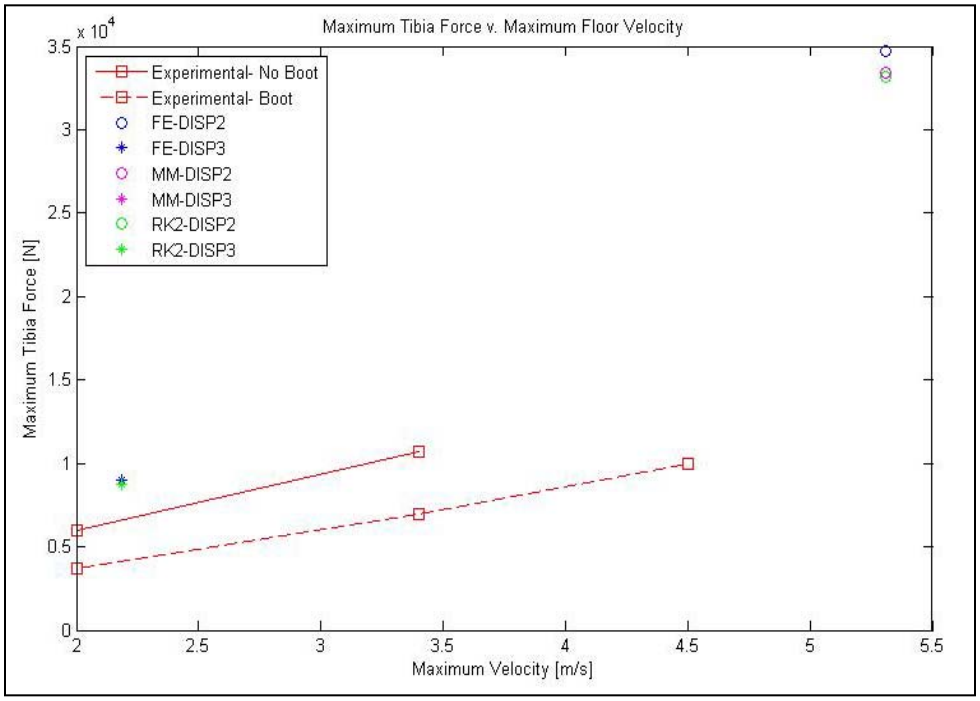

Figure 7. Scaled maximum tibia force versus maximum floor velocity.

4. GUI Executable

In order to make the computation more user-friendly, a graphical user interface (GUI) executable was developed to allow the user to reproduce the results of this report without extensive knowledge of the code. A screenshot is provided in figure 8, showing the results of using Bir et al. (2006) Condition 1 TROSS data.

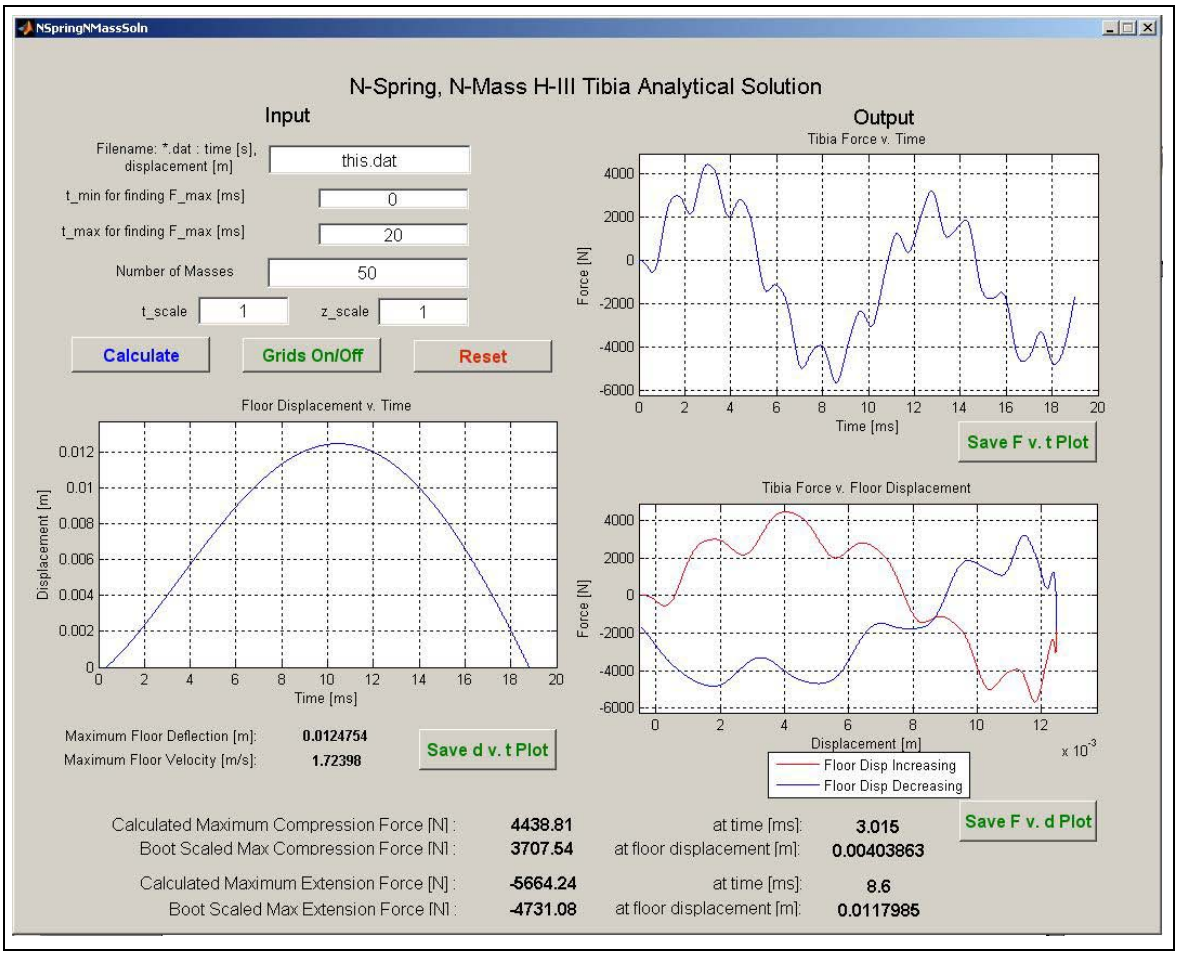

Figure 8. GUI executable screenshot.

To improve the accuracy of the predicted tibia force, the model was extended further to include the presence of the ankle and foot, and the boot. The parameters listed in table 3, derived from the Hybrid-III LS-DYNA model, were used in the calculation of the tibia force.

Table 3. Lengths and spring constants of the H-III tibia, ankle/foot, and boot.

	Tibia	**Ankle/Foot**	**Boot**
Length (m)	0.4523	0.06119	0.02967
Spring Constant (N/m)	26,954,124.92	k_{tibia}	2,898,600

The values for the spring constants of the ankle and foot and of the boot are approximated. The assumption that the spring constant of the ankle was equal to the spring constant of the tibia is nearly arbitrary; the spring constant of the boot assumes a hard ethylene propylene diene monomer (EPDM) rubber of 8.6 MPa at 100% elongation and a cross-sectional area of 0.01 m^2.

The mass parameters—m_{femur}, m_{tibia}, and m_{foot}—are shown in table 4.

Table 4. Masses of the Hybrid-III femur, tibia, and foot.

m_{femur} (kg)	4.16503
m_{tibia} (kg) (includes ankle)	2.44792
m_{foot} (kg) (includes boot)	1.38669

With this further modification, the model places a mass at the ankle and at the heel and provides a different spring constant for both the ankle and the sole of the boot. The significantly lower spring constant of the EPDM rubber in the sole compared to the bone structures greatly diminished the axial tibia force.

For force verification purposes, an effort to match the maximum floor displacements and velocities to the experimental values, the TROSS data from Bir et al. (2006) is recreated manually from the paper through measurements and extrapolations. The predicted force versus time for condition 1 is shown in figure 9.

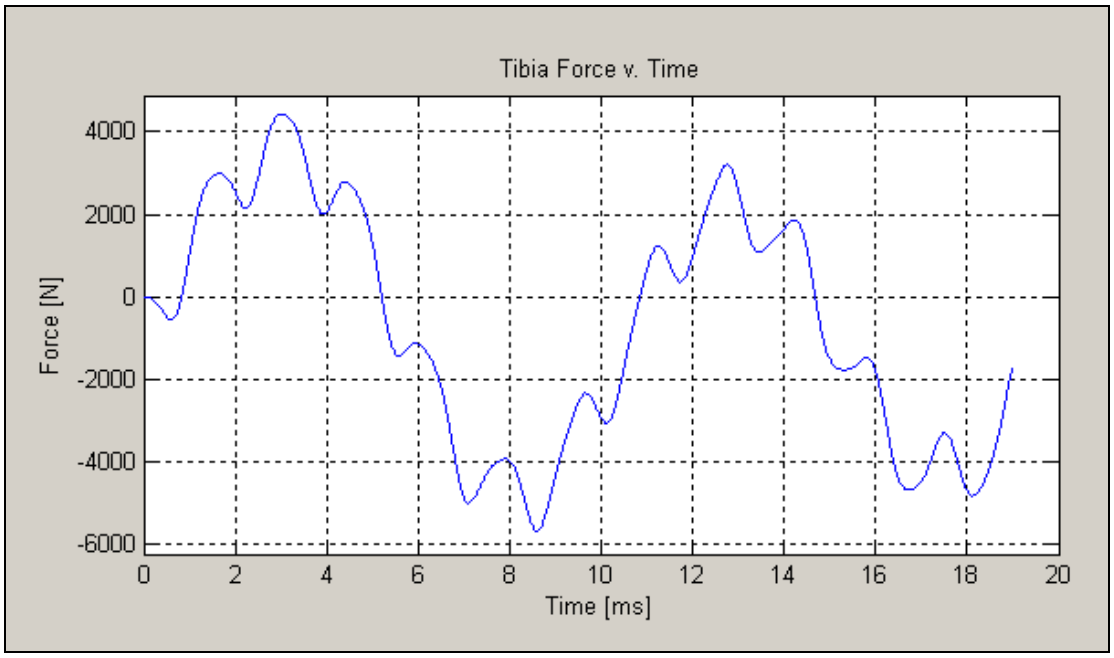

Figure 9. Calculated tibia force versus time for Bir et al. (2006) condition 1.

Repeating the calculation for each of the conditions provided in Bir et al. (2006) resulted in a more accurate approximation of the calculated tibia force using a 50-spring, 50-mass model (table 5).

Table 5. Results from the model using Bir et al. (2006) conditions 1 to 3 floor displacement inputs.

Condition	Max Floor Displacement (m)	Max Floor Velocity (m/s)	Calculated Max Tibia Force (N)	Experimental Max Tibia Force (N)	Error = (Calculated – Experimental) / Experimental
1	0.0125	1.7	4439	3709	0.20
2	0.0218	3.3	8148	7000	0.16
3	0.0269	4.3	10800	9984	0.08

Since the model includes boots, the results in table 5 are compared to the experimental results for conditions 1 to 3. From the results, a scaling factor (experimental/predicted) is calculated for each condition and a quadratic polynomial is used to relate the scaling factor to its corresponding maximum floor displacement and maximum floor velocity. This polynomial should be further improved through the verification of more data points.

Since the scaling factor produced using the maximum floor velocity over-predicts the maximum tibia force as seen in figure 10, these scaling factors are used in the model to provide a conservative estimate.

It can be seen in figures 10 and 11 that the model with modifications to account for the properties of the ankle, foot, and boot results in a more accurate prediction of the axial tibia force. Since the

correlation between the experimental data and the scaled analytical solution is stronger using the maximum floor velocity, the GUI presents the scaled analytical solution using the scaling factor determined by the maximum floor velocity.

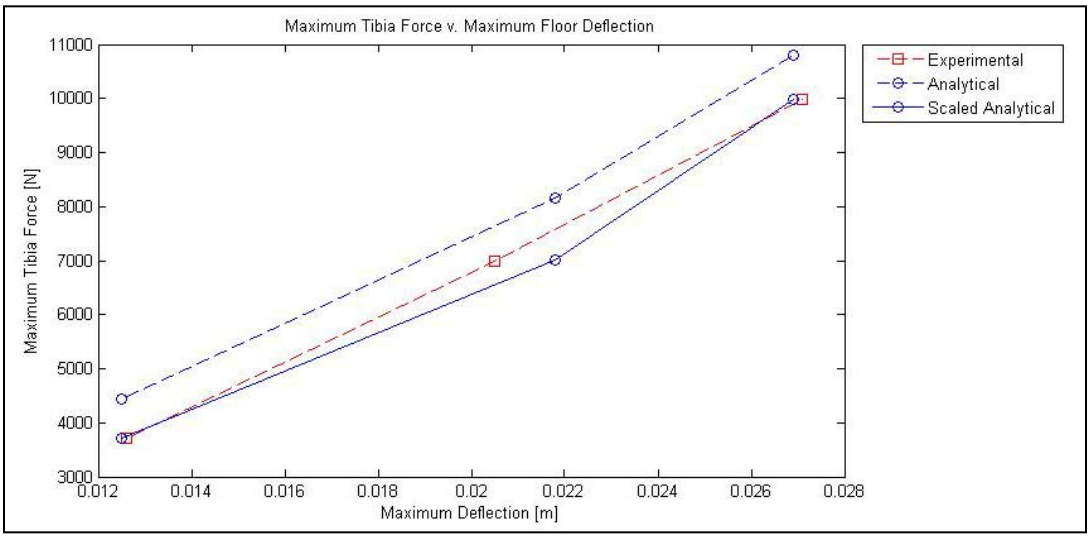

Figure 10. Boot maximum tibia force versus maximum floor displacement.

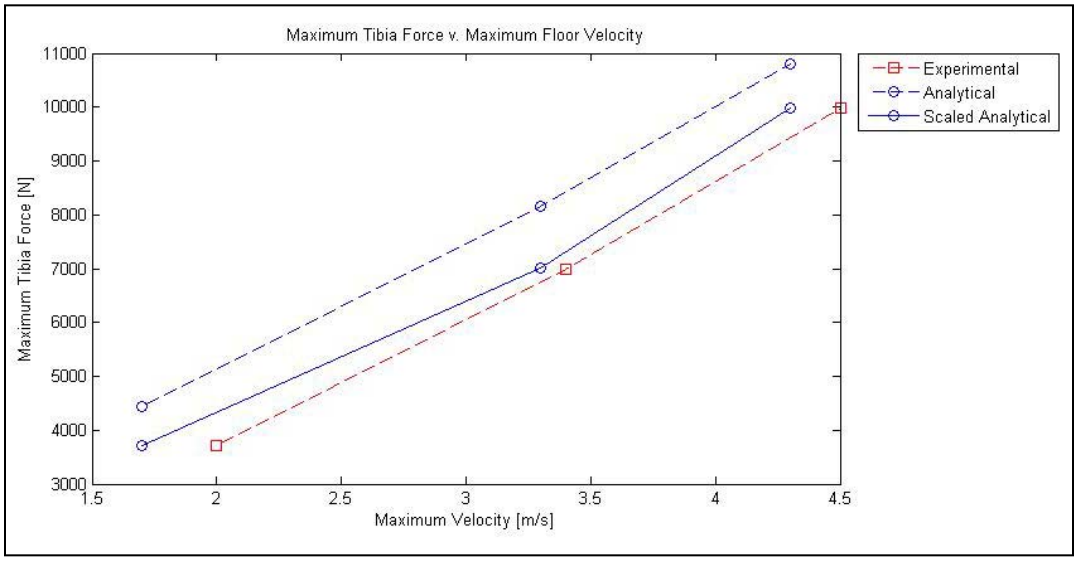

Figure 11. Boot maximum tibia force versus maximum floor velocity.

5. Summary and Conclusions

The one-dimensional n-spring analytical model given simulated floor displacement data produced maximum tibia forces within the same magnitude of the experimental data. Using the forward Euler, midpoint method, and two-step Runge-Kutta numerical integration methods, the

developed script calculated a numerical solution for the tibia force given the floor displacement over time. A scaling factor dependent on the maximum floor velocity was applied to obtain analytical results that very nearly matched the experimental results. While the model has been validated with the experimental data presented in Bir et al. (2006), further verification of the model with a larger data set is necessary.

6. References

Bir, C.; Barbir, A.; Wilhelm, M.; van der Horst, M.; Dosquet, F.; Wolfe, G. Validation of Lower Limb Surrogates as Injury Assessment Tools in Floor Impacts due to Anti-Vehicular Land Mines. *IRCOBI Conference*, Madrid, Spain, September 2006.

Appendix A. Figures Referenced from Bir et al. (2006)

Table A-1. Results from testing conducted using TROSS system and Hybrid-III surrogate.

Hybrid III	Plate displacement (mm)	Peak plate velocity (m/s)	Tibia Force - Z (N)
Condition 1 no boot	12.3	2.0	5970
Condition 1 boot	12.6	2.0	3709
Condition 2 no boot	21.8	3.4	10740
Condition 2 boot	20.5	3.4	7000
Condition 3 boot	27.1	4.5	9984

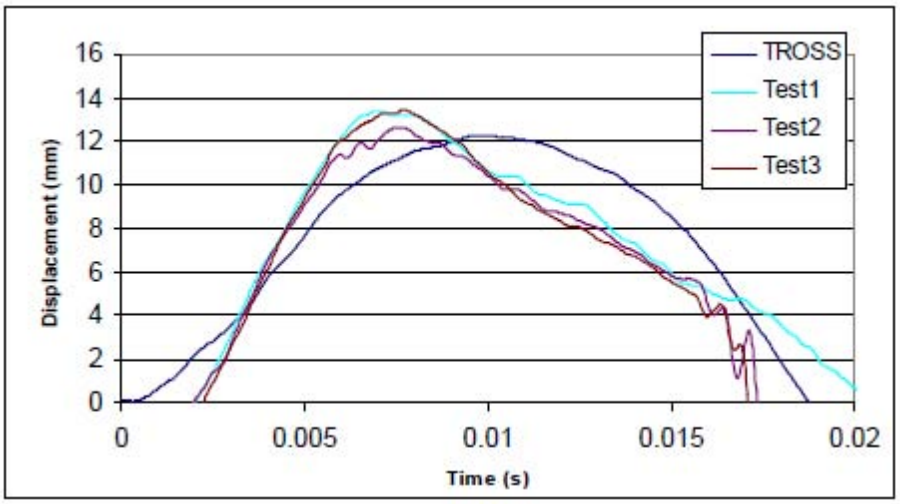

Figure A-1. Comparison of linear impactor data with TROSS testing using Hybrid-III lower limb for Condition 1.

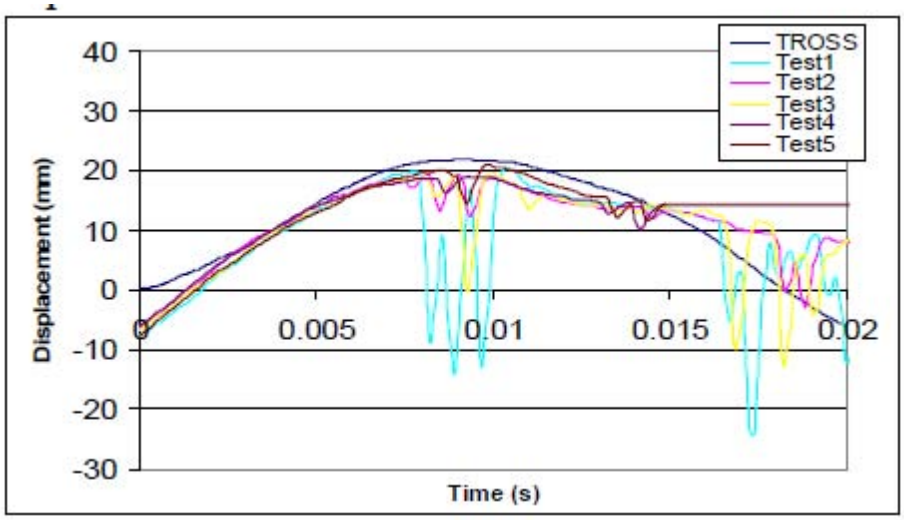

Figure A-2. Comparison of linear impactor data with TROSS testing using Hybrid-III lower limb for Condition 2.

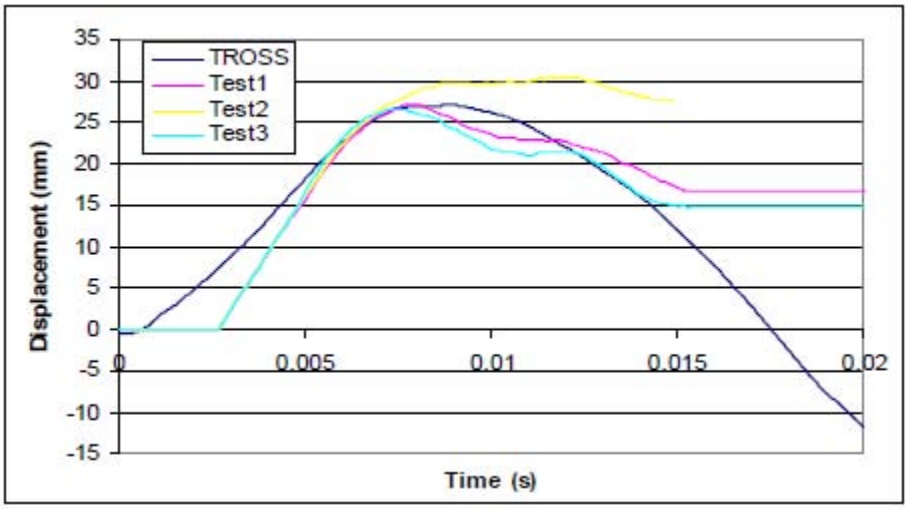

Figure A-3. Comparison of linear impactor data with TROSS testing using Hybrid-III lower limb for Condition 3.

NO. OF COPIES ORGANIZATION

1 ELEC ADMNSTR
DEFNS TECHL INFO CTR
ATTN DTIC OCP
8725 JOHN J KINGMAN RD STE 0944
FT BELVOIR VA 22060-6218

3 US ARMY RSRCH LAB
ATTN IMNE ALC HRR
MAIL & RECORDS MGMT
ATTN RDRL CIM L TECHL LIB
ATTN RDRL CIM P TECHL PUB
ADELPHI MD

1 CD OFC OF THE SECY OF DEFNS
ATTN ODDRE (R&AT)
THE PENTAGON
WASHINGTON DC 20301-3080

1 US ARMY INFO SYS ENGRG CMND
ATTN AMSEL IE TD A RIVERA
FT HUACHUCA AZ 85613-5300

1 COMMANDER
US ARMY RDECOM
ATTN AMSRD AMR
W C MCCORKLE
5400 FOWLER RD
REDSTONE ARSENAL AL
35898-5000

2 US ARMY RESEARCH OFC
D STEPP
B LAMATTINA
PO BOX 12211
RESEARCH TRIANGLE PARK NC
27709-2211

5 DARPA
ATTN IXO S WELBY
SPECIAL PROJECTS OFC
A ALVING
TACTICAL TECHNOLOGY OFC
W JOHNSON
DEFENSE SCIENCE OFC
S WAX
ADVANCED TECHNOLOGY OFC
D HONEY
3701 N FAIRFAX DR
ARLINGTON VA 22203-1714

NO. OF COPIES ORGANIZATION

1 DIR
DTRA
MSC 6201
8725 JOHN J KINGMAN RD
FORT BELVOIR VA 22060-6201

1 DIR
DEFENSE INTELLIGENCE AGENCY
TA 5
K CRELLING
WASHINGTON DC 20310

1 COMMANDER
US ARMY MATERIEL CMD
AMSMI INT
9301 CHAPESK RD
FT BELVOIR VA 22060-5527

1 COMMANDER
US ARMY TACOM
PM COMBAT SYSTEMS
SFAE GCS CS
6501 ELEVEN MILE RD
WARREN MI 48397-5000

4 PM FCS BCT MSI
SFAE GCS UA
J PARKER
P CAG
S GRIEG
T MCKHEEN
6501 ELEVEN MILE RD
WARREN MI 48397-5000

1 COMMANDER
US ARMY TACOM
PEO CS & CSS
PM LIGHT TACTICAL VHCLS
SFAE CSS LT M1114 MGR
6501 ELEVEN MILE RD
WARREN MI 48397-5000

1 COMMANDER
US ARMY AMCOM
AVIATION APPLIED TECH DIR
J SCHUCK
FT EUSTIS VA 23604-5577

NO. OF COPIES ORGANIZATION

5 COMMANDER
NAVAL SURFACE WARFARE CTR
CARDEROCK DIVISION
R PETERSON CODE 2120
R CRANE CODE 6553
T BURTON CODE 667
U SORATHIA
C WILLIAMS CODE 6551
9500 MACARTHER BLVD
WEST BETHESDA MD 20817-5700

13 COMMANDER
US ARMY TACOM
AMSTA TR R
S KNOTT
D DICESURE
J BENNETT
D HANSEN
AMSTA JSK
E BARSHAW
M CHAIT
D TEMPLETON
L FRANKS
AMSTA TR D
D OSTBERG
L HINOJOSA
S HODGES
C FILAR
AMSTA CS SF
F SCHWARZ
WARREN MI 48397-5000

1 OFC OF NAVAL RESEARCH
J KELLY
3701 N FAIRFAX DR
ARLINGTON VA 22203-1714

1 CD EXPEDITIONARY WARFARE
DIV N85
F SHOUP
2000 NAVY PENTAGON
WASHINGTON DC 20350-2000

1 MARINE CORPS SYSTEM CMD
J BURNS
2200 LESTER ST
QUANTICO VA 22134

1 CENTRAL INTELLIGENCE AGENCY
WINPAC/CWTG/GWET
M DAN
RM 4P07 NHB
WASHINGTON DC 20505

NO. OF COPIES ORGANIZATION

1 DIR
LANL
F ADDESSIO MS B216
PO BOX 1633
LOS ALAMOS NM 87545

2 THE BOEING CO
J CHILDRESS
N GERKEN
MS 84-69 CAGE CODE 81205
PO BOX 3707
SEATTLE WA 98124

3 BAE SYSTEMS
G THOMAS
T PIKE
M IWEN
PO BOX 359 CAGE CODE 80212
SANTA CLARA CA 95050

3 BAE SYSTEMS
R BRYNSVOLD
W BALLATA
J BRODY
PO BOX 21099
MINNEAPOLIS MN 55421

2 BAE SYSTEMS
T STEELE
R SCIORTINO
CAGE CODE 06085
PO BOX 15512
YORK PA 17405-1512

2 GDLS
G TEAL
B CALDWELL
PO BOX 1800
WARREN MI 48090-1800

1 US ARMY TANK-AUTOMOTIVE
RESEARCH DEVELOPMENT AND
ENGINEERING CENTER
EMERGING TECHNOLOGIES
RICHARD GOETZ
AMSRD TAR R MS 263
WARREN MI 48397-5000

2 GDLS
J ERIDON
T ZELEZNIK
STERLING HEIGHTS COMPLEX
38500 MOUND ROAD
STERLING HEIGHTS MI 48310-3200

NO. OF
COPIES ORGANIZATION

2 MARINE CORPS SCIENCE & TECH
OFFICE OF NAVAL RESEARCH
L MASTROIANNI
J BRADEL
ONE LIBERTY CENTER
875 N RANDOLPH ST STE 1156B
CODE 30
ARLINGTON VA 22203-1995

1 SHIP HULL MECHANICAL &
ELECTRICAL S&T DIV
OFFICE OF NAVAL RESEARCH
ROSHDY GEORGE S BARSOUM PHD
PE ONR334
800 N QUINCY ST
ARLINGTON VA 22217-5660

1 US ARMY RSRCH LAB
ATTN RDRL CIM G T LANDFRIED
BLDG 4600
ABERDEEN PROVING GROUND MD
21005-5066

NO. OF
COPIES ORGANIZATION

ABERDEEN PROVING GROUND

2 DIR USARL
AMSRD ARL CI LP (BLDG 305)

71 DIR
US ARMY RESEARCH LAB
RDRL LOA F
M ADAMSON
RDRL SER E
S MCKNIGHT
RDRL SLB A
P KUSS
J PLOSKONKA
E HUNT
B WARD
RDRL SLB D
R GROTE
J POLESNE
RDRL SLB E
E FIORAVANTE
RDRL VTR R
J BORNSTEIN
RDRL WM
L BURTON
J SMITH
RDRL WMM A
M MAHER
S GHIORSE
J WOLBERT
RDRL WMM B
M VANLANDINGHAM
RDRL WMM B
T BOGETTI
B CHEESEMAN
J CLAYTON
B LOVE
R DOOLEY
C FOUNTZOULAS
C YEN
RDRL WMM C
R JENSEN
RDRL WMM D
E CHIN
J LASALVIA
J SANDS
RDRL WMM E
J CAMPBELL
P DEHMER
T JESSEN
G GILDE
P PATEL
S WALSH
RDRL WWM F
K DOHERTY
J MONTGOMERY

NO. OF
COPIES ORGANIZATION

RDRL WML
M ZOLTOSKI
J NEWILL
RDRL WML G
W DRYSDALE
RDRL WMT C
R COATES
RDRL WMP
P BAKER
S SCHOENFELD
RDRL WMP A
B RINGERS
RDRL WMP B
C HOPPEL
B LEAVY
RDRL WMP C
T BJERKE
RDRL WMP D
T HAVEL
V HERNANDEZ
S HUG
M KEELE
D KLEPONIS
J RUNYEON
B SCOTT
RDRL WMP E
M BURKINS
W GOOCH
D HACKBARTH
E HORWATH
M KLUSEWITZ
C KRAUTHAUSER
M LOVE
RDRL WMP F
R BITTING
D FOX
A FRYDMAN
N GNIAZDOWSKI
R GUPTA
X HUANG
RDRL WMP G
N ELDREDGE
S KUKUCK
RDRL WMP H
T FARRAND
E KENNEDY
L MAGNESS
B SORENSEN

TOTAL: 139 (1 ELEC, 2 CDS, 136 HCs)